Journal of Physics: Conference Series

PAPER • **OPEN ACCESS**

Computational and experimental study of 3D flow near the cube immersed in the turbulent free convection boundary layer on a vertical heated plate

To cite this article: Yu S Chumakov *et al* 2020 *J. Phys.: Conf. Ser.* **1675** 012023

Computational and experimental study of 3D flow near the cube immersed in the turbulent free convection boundary layer on a vertical heated plate

Yu S Chumakov, A M Levchenya and E M Smirnov

Higher School of Applied Mathematics and Computational Physics,
Peter the Great St. Petersburg Polytechnic University,
29 Polytechnicheskaya Street, St. Petersburg, 195251 Russia

E-mail: levchenya_am@spbstu.ru

Abstract. Results of a coordinated computational and experimental study of time-averaged velocity and temperature fields in the vicinity of an adiabatic cube that is inserted into the turbulent free convection vertical-plate boundary layer are presented. The numerical simulation was based on the steady-state RANS approach using the *k*-ω SST turbulence model and a version of the differential Reynolds stress model (DRSM). The hot-wire technique was used for velocity measurements, simultaneously with temperature measurements by an accompanied "cold" wire. Two turbulence models produced similar vortex flow structures near the obstacle; however some important quantitative distinctions were observed. The velocity value profiles predicted for the middle vertical plane showed generally a good accordance with the hot-wire measurements carried out in this plane, especially in the DRSM case.

1. Introduction

A huge effort has been made to study flow dynamics and heat transfer in the generic case of the statistically 2D turbulent free convection boundary layer (FCBL) developing on a vertical heated flat plate. However, at certain conditions, a series of protuberances (or a single protuberance) can be mounted on the heated plate. Examples are structural elements of industrial devices or obstacles specially introduced to achieve heat transfer augmentation (see, for instance, [1]).

Results of RANS *k*-ω SST numerical simulation of 3D turbulent flow and heat transfer near a finite-height circular cylinder disturbing the turbulent FCBL are reported in [2], with a special attention to the influence of the height-to-diameter ratio on skin friction and augmented heat transfer patterns in the front and in the rear of the obstacle. Hot-wire measurements of the turbulent FCBL velocity field disturbed by a circular cylinder mounted on a heated plate were carried out recently in [3]. A comparison with the simulation data reported in [2] has shown in particular that the *k*-ω SST model overestimates considerably the length of the FCBL recovering region behind the obstacle.

The present paper covers results of a coordinated computational and experimental study of time-averaged velocity and temperature fields in the vicinity of an adiabatic cube that is inserted into the turbulent free-convection boundary layer developing along a vertical heated plate. The numerical simulation was based on the steady-state RANS approach using the *k*-ω SST turbulence model and a version of the differential Reynolds stress model. The hot-wire technique was used for velocity measurements, simultaneously with temperature measurements by an accompanied "cold" wire.

2. Numerical simulation

Figure 1a illustrates the flow configuration considered. A cube of size a mounted on a vertical plate, kept at constant temperature T_w, disturbs the incoming turbulent FCBL. It is assumed that the ambient temperature T_a is less than T_w, and $(T_w-T_a)/T_a<<1$. The x-axis of the used Cartesian system is directed vertically upward; and xz-planes are parallel to the plate. The x-coordinate is counted from the cube centre.

The local state of the incoming (undisturbed) two-dimensional layer can be characterized by the Grashof number, $Gr_\delta=g\beta_T(T_w-T_a)\delta^3/\nu^2$, based on a characteristic local thickness of the layer, δ. The thickness δ is defined as integral of the normalized streamwise velocity profile, u/u_{max}, from the plate surface (y=0) to $y=\delta_T$, where δ_T is the thermal boundary layer thickness evaluated as a distance from the plate where the fluid temperature differs from T_a by 1% of (T_w-T_a).

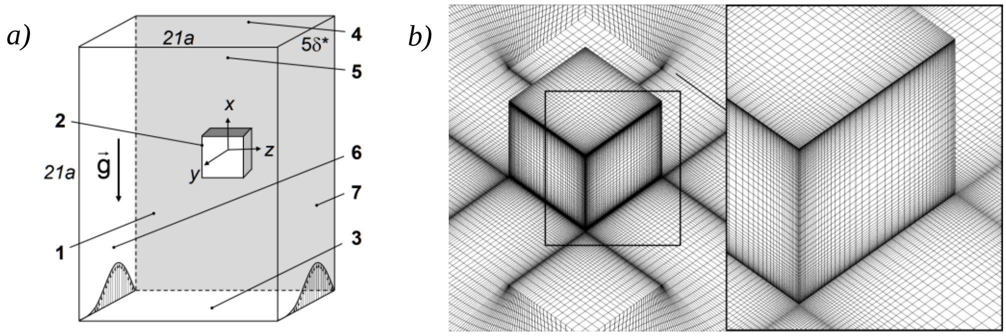

Figure 1. (a) Flow domain and boundaries, (b) computational grid in the vicinity of the cube.

It is assumed that the cubical obstacle is placed at a position, where $\delta=\delta^*$ in the case with no obstacle. Correspondingly, the simulated flow is determined by three dimensionless parameters. These are the ratio of the layer thickness to the cube size, $\beta^*=\delta^*/a$, the Grashof number Gr_δ^* based on δ^*, and the Prandtl number, Pr. The present simulation deals with the case of $\beta^*=3/2$, $Gr_\delta^*=10^6$ and Pr=0.7.

The computational domain used (Figure 1a) has a form of a parallelepiped. The cube centre is positioned in the domain middle (vertical) plane, at a distance of $10.5a$ from the inlet section. The computational domain size is $21a\times5\delta^*\times21a$ m in x-, y- and z-direction, respectively.

The no-slip condition is imposed at the plate (1 in Figure 1a) and at the cube surface (2). The cube is treated as adiabatic. Inlet profiles of velocity, temperature and turbulence characteristics, prescribed at the inlet section (3), are obtained from 2D RANS simulation of the incoming turbulent FCBL that is carried out with the same turbulence model (details can be found elsewhere [2]). A generalized inflow/outflow ("pressure-outlet") condition is applied for the outlet section (4). The "pressure-inlet" condition is used at the external plane (5) parallel to the plate. Symmetry conditions are prescribed at the boundaries confining the calculation domain in the spanwise direction (6, 7).

The flow dynamics and heat transfer are described by the RANS and energy equations. The Boussinesq approach is adopted to incorporate the buoyancy action. The k-ω SST model and the BSL version of the Differential Reynolds Stress Model (denoted below as DRSM) [4], as implemented in ANSYS Fluent 18.2, are used for turbulence modelling. The turbulent Prandtl number is set to 0.85.

The used 3D computational grid consisted of about 4 million cells. The average normalized distance from the centre of the first computational cell to the wall, Y^+, was of about 0.2. A special attention was paid to achieve a good grid resolution near the cube edges (Figure 1b). Numerical solutions were obtained with the second-order scheme for convective flux evaluation in all governing equations (momentum, energy and turbulence parameter transport equations). For both turbulence models, the flow predicted were steady-state and symmetrical with respect to the mid vertical plane.

For the DRSM case, Figure 2 presents the predicted 3D flow pattern with specific vortex structures in the front and in the rear of the obstacle. Despite the SST model and the DRSM predict similar flow structures, there are some notable distinctions in quantitative characteristics of the disturbing action of the obstacle, as illustrated below. Note that the superscript (0) marks a value corresponding to the undisturbed 2D FCBL case.

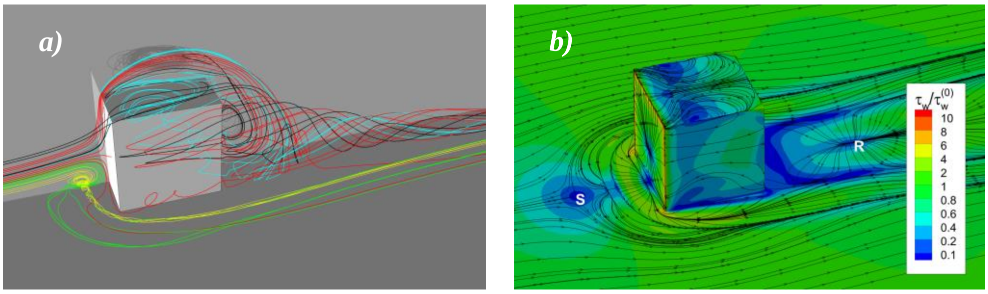

Figure 2. 3D flow structure predicted with the DRSM model: (a) volume streamline pattern, (b) surface streamlines superimposed on the normalized wall shear stress distributions.

Figure 3 shows mid-plane distributions of velocity value, U=sqrt(u^2+v^2), and temperature predicted with two turbulence models. The velocity value is normalized with the maximal velocity at the section positioned at a distance of 2.8a from the front face of the cube, where the FCBL can be treated as undisturbed. The normalized temperature,θ, is defined as $\theta=(T-T_a)/(T_w-T_a)$. Velocity maps also cover streamline patterns and insertions with a magnified view of the front separation zone, where the horseshoe-shaped vortex structure originates. It is seen that the DRSM predicts a shorter separation zone upstream of the obstacle, as compared with the SST model. It is noteworthy that the recirculation zone in the rear of the cube is also smaller in the DRSM case. Comparing the temperature distributions, one can conclude that the SST model predicts a thicker temperature layer.

Predicted distributions of the normalized plate-surface shear stress and heat flux are presented in Figure 4. In addition, limiting streamline patterns are shown in the shear stress maps. When comparing images of the horseshoe vortices “footprints” obtained with two models, one can conclude that generally the SST model predicts a larger size of the FCBL zone disturbed by the obstacle.

a) 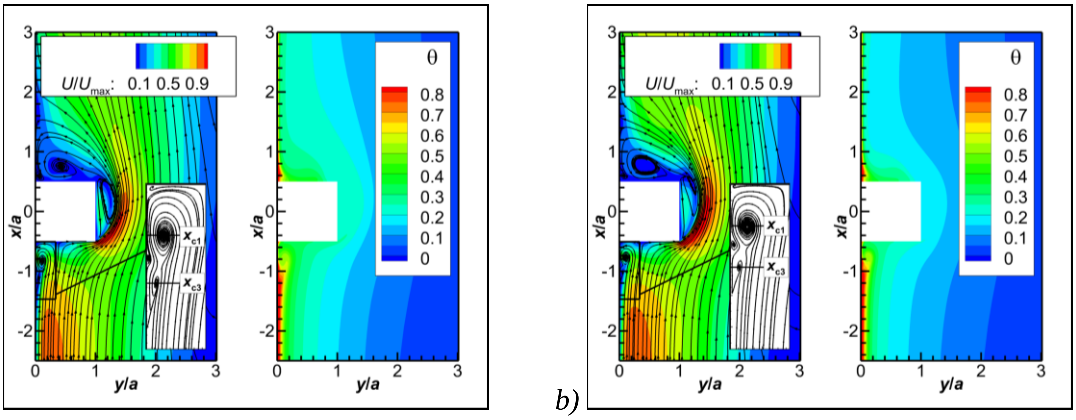 b)

Figure 3. Midplane velocity and temperature distributions: (a) k-ω SST, (b) DRSM.

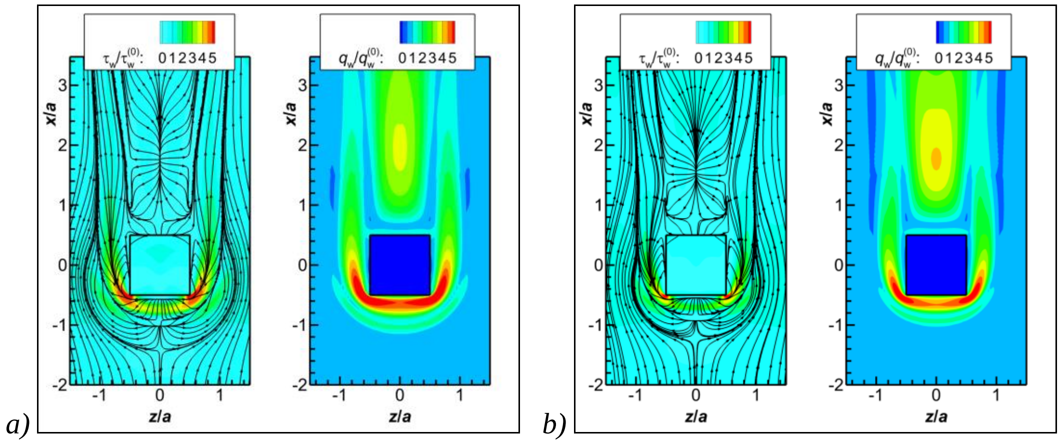

Figure 4. Plate-surface shear stress and heat flux distributions: (a) k-ω SST, (b) DRSM.

Some representative characteristics of flow and heat transfer are summarized in Table 1. The table includes: maximal normalized values of shear stress and heat flux on the plate surface, the coordinate of flow separation in front of the obstacle, x_S (point S in Figure 2b), the position of the main horseshoe vortex center, x_{c1} (shown in Figure 3), the position of the tertiary horseshoe vortex center, x_{c3} (shown also in Figure 3), and the position of the flow reattachment point downstream of an obstacle, x_R (point R in Figure 2b).

Table 1. Flow and heat transfer characteristics predicted with two RANS models.

Turbulence model	$\max(\tau_w/\tau_w^{(0)})$	$\max(q_w/q_w^{(0)})$	x_S/a	x_{c1}/a	x_{c3}/a	x_R/a
k-ω SST	9.39	6.70	-1.423	-0.822	-1.128	1.764
DRSM	7.53	5.82	-1.239	-0.765	-1.025	1.540

Comparing to the SST model, a peak value of the plate-surface heat flux predicted in the DRSM case is about 25% lower, and maximum of wall shear stress is also lower, by about 15%. These findings correlate to smaller characteristic dimensions (10-15% decrease) of horseshoe and near-wake vortex structures obtained in the DRSM calculations.

3. Experimental facility and conditions

Experiments were carried out using a laboratory rig created at the Saint-Petersburg Polytechnic University in the nineties [5] for studies of transitional and turbulent FCBL developing along a heated vertical plate. Last time the rig was updated to improve the heated-surface temperature control. Free convection of air develops along an aluminum plate with 4.95 m height and 0.88 m width (Figure 5a). The plate is heated by 25 independently-controlled heaters.

Disturbing action of a cubical obstacle on the nominally 2D turbulent FCDL was investigated under conditions that were close to those adopted in the above-described numerical simulation. A nearly adiabatic cube, 40 mm size, was mounted on the plate midline at a distance of $x' \equiv x - x_{LE} = 1.8$ m from the plate leading edge (LE). The plate was kept at a constant temperature of 60°±0.5°C. The ambient (external) temperature was 26±1°C. Under this thermal conditions, the characteristic thickness δ of the undisturbed FCBL measured at x'=1.8 m (the cube position) was evaluated as $\delta^*=60\pm3$ mm, and, correspondingly, the ratio $\beta^*=\delta^*/a$ was estimated as 3/2 with an uncertainty of 5%. The Grashof number Gr_{δ}^* was estimated as $0.9\cdot10^6$ with an uncertainty of 15%.

The present experiments were limited by hot-wire measurements of the mean temperature and the velocity value distributions over the middle plane (Figure 5b). A two-wire probe was used, with a hot wolfram wire for velocity measurement and a "cold" wolfram wire for temperature measurements; both wires had 5 μm diameter and 3.5 mm length. The distance between the wires was 2 mm. Using a coordinates device, the probe could be shifted both along the plate (x-coordinate) and normal to the plate (y-coordinate). Uncertainties of positioning of the probe wires were evaluated as 0.5 mm for the x-coordinate and 20 µm for the y-coordinate.

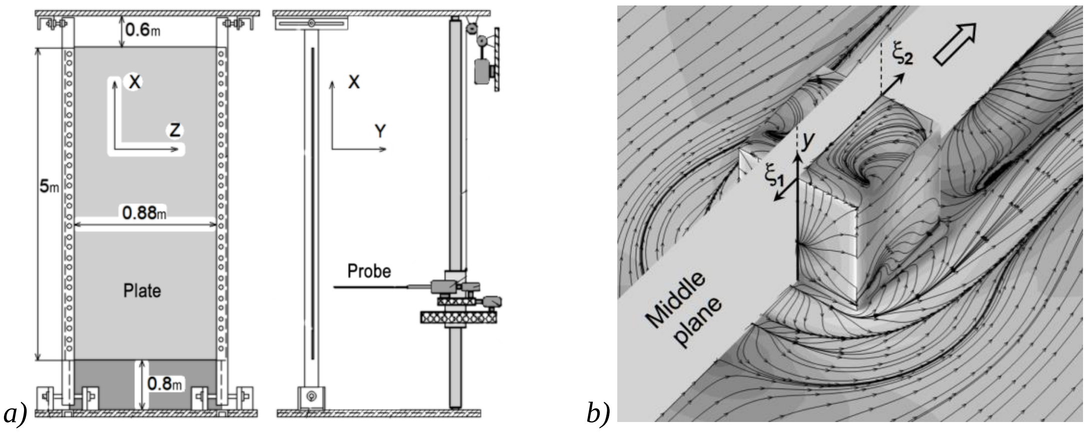

Figure 5. (a) Experimental rig scheme, (b) auxiliary coordinates in the measurement plane.

For the hot-wire velocity measurements, it is well known that the measured velocity of air near the wall is influenced by the wall-proximity effects. In particular, Tsuji and Nagano [6] have illustrated that in case of the 2D turbulent FCBL the wall-proximity effects covered a layer of about 1 mm thickness. To be sure that the present results of our measurements in the disturbed FCBL are not influenced by the wall proximity, the data obtained at y<2 mm have been omitted.

4. Comparison of simulation and measurement data

For several sections positioned upstream of the obstacle, Figure 6 shows the predicted velocity and temperature profiles versus the measurement data. The coordinate ξ_1 (see Figure 5b) defines the distance from the front face of the cube to a section considered. One can see that two turbulence models produce close results, and a considerable distinction between the numerical and experimental velocity data is observed only at $y/a<0.1$ ($y<4$ mm) for two sections: ξ_1 = 11 and 16 mm. Figure 3 shows that a reverse flow forms near the plate at these sections due to formation of the horseshoe vortex. In the reality this vortex can perform spatial oscillations, which are not reproduced in the RANS simulation. On the other hand, the hot-wire measurements with the above-described probe hardly have high accuracy for this relatively small zone of local reverse flow. All this needs further investigation.

Measured temperature profiles do not change their form considerably when approaching the cube, except for the case of ξ_1 = 4 mm. It is in contrast with the simulation, where the action of the predicted stationary horseshoe vortex results in a pronounced deformation of the temperature field. It seems that an adequate temperature field upstream of the obstacle can be predicted only with an unsteady eddy-resolving approach [7].

Figure 7 presents a comparison of the calculated and measured profiles of velocity value and temperature behind the obstacle. Positions of different sections with respect to the back face of the cube is defined by the ξ_2-coordinate (see Figure 5b). It is remarkable that in the near-wake region, the velocity profiles predicted with the SST model are in a better accordance with the measurements, as compared with the DRSM case, whereas the Reynolds stresses model shows a pronounced superiority in the far wake, at ξ_2/a >2. It is also seen in Figure 8, where variations of $U(y/a=0.3)$ versus ξ_1 (upstream of the cube) or ξ_2 (behind the obstacle) are illustrated.

For the temperature filed behind the cube, one can see again that, compared to the measurements, the RANS-based simulation predicts stronger deviations of temperature profiles from the profile typical for the undisturbed FCBL.

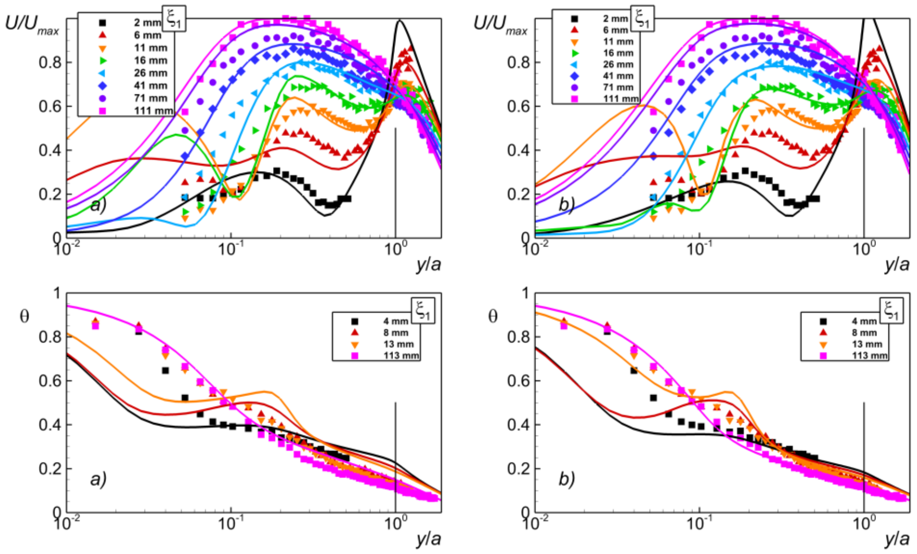

Figure 6. Predicted velocity and temperature profiles upstream of the obstacle versus the measurement data: (a) *k*-ω SST, (b) DRSM.

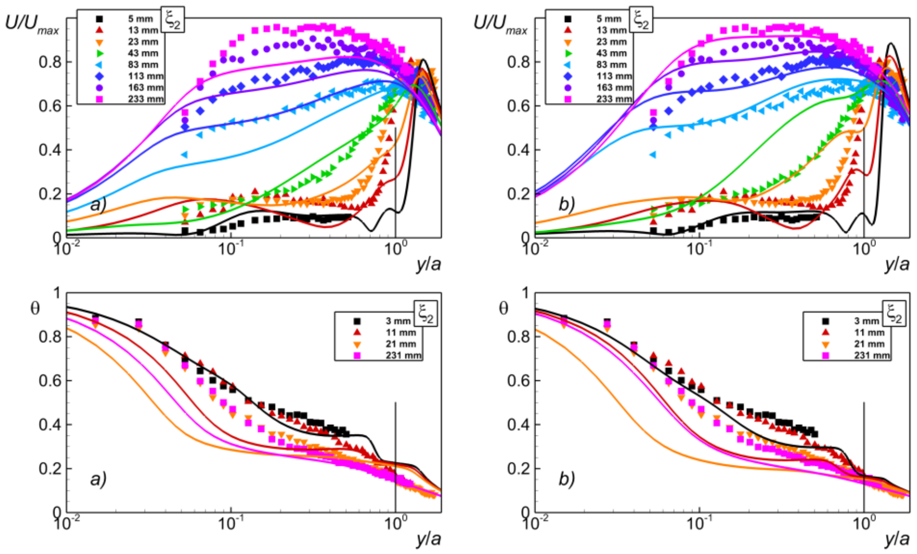

Figure 7. Predicted velocity and temperature profiles behind the obstacle versus the measurement data: (a) *k*-ω SST, (b) DRSM.

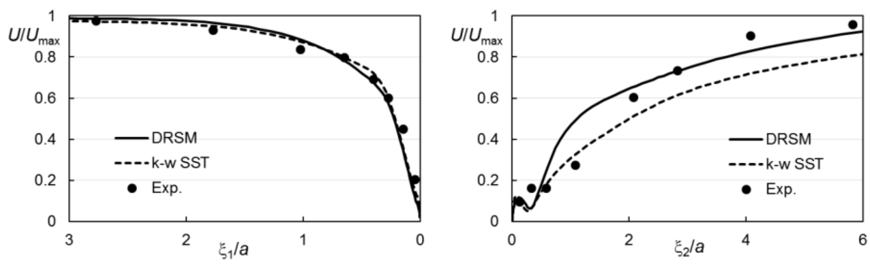

Figure 8. Longitudinal distribution of mid-plane velocity taken at y/a=0.3.

Conclusions

A computational and experimental study of 3D flow near a plate-mounted cubical obstacle disturbing the turbulent FCBL has been carried out. The k-ω SST model and the differential Reynolds stress model (DRSM) used for steady-state RANS computations produce similar vortex flow structures near the obstacle; however there are some important quantitative distinctions. The DRSM predicts a shorter separation zone upstream of the obstacle, where a system of horseshoe-shaped vortex structures is formed. The recirculation zone in the rear of the cube is also smaller in the DRSM case. The velocity value profiles predicted for the mid-plane are generally in a good accordance with the hot-wire measurements carried out in this plane, especially in the DRSM case. Measured temperature profiles do not change their form considerably when approaching the obstacle that is in contrast with the simulation predicting a pronounced deformation of the temperature field due to action of the stationary horseshoe vortex. It gives a motivation for using eddy-resolving approaches in the future.

Acknowledgments

The study is supported by the Russian Science Foundation under grants no. 18-19-00082.

References

[1] Tsuji T, Kajitani T and Nishino T 2007 *Int. J. of Heat and Fluid Flow* **28** 1472–83
[2] Smirnov E M, Levchenya A, Zhukovskaya V 2019 *Int.J. Heat Mass Transfer* **144** 118573–84
[3] Chumakov Yu S, Levchenya A, Khrapunov E 2020 *SPbSPU J.Phys.Math.* **13**(1) 66–77
[4] Wilcox D C 1993 *Turbulence modeling for CFD* (Glendale: Griffin Printing) p 460
[5] Chumakov Yu S 1999 *High temperature* **37**(5) 714–9
[6] Tsuji T and Nagano Y 1988 *Int. J. Heat Mass Transfer* **31** 1723–34
[7] Levchenya A, Kolesnik E, Smirnov E M 2019 *J. Phys.: Conf. Ser.* **1400** 077031-6